

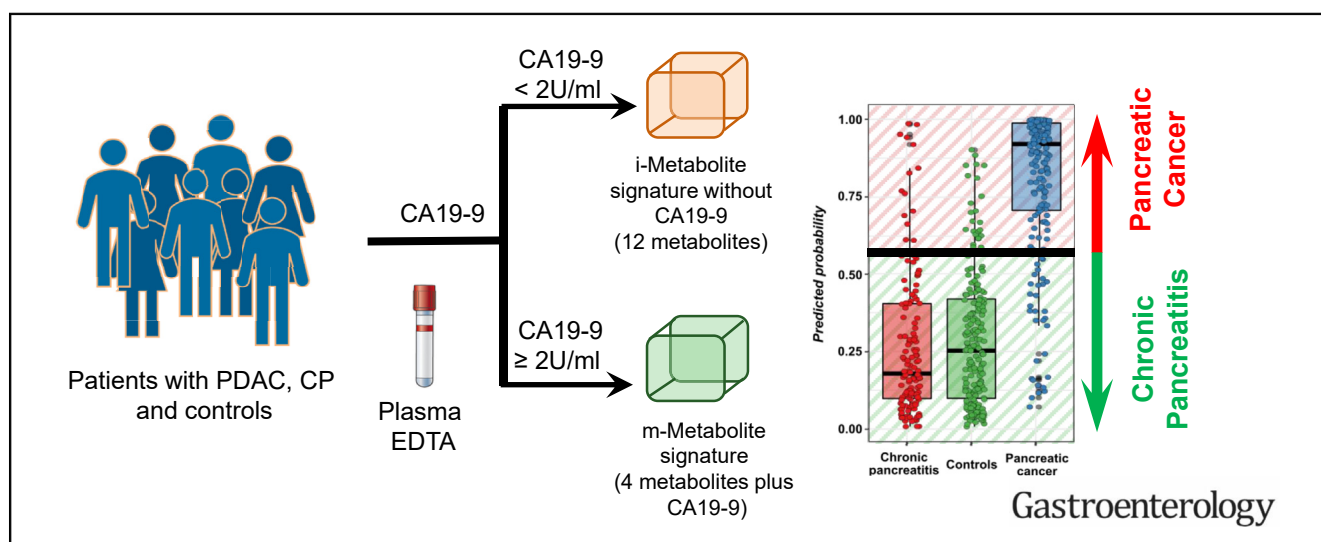
PANCREAS

Independent Validation and Assay Standardization of Improved Metabolic Biomarker Signature to Differentiate Pancreatic Ductal Adenocarcinoma From Chronic Pancreatitis



Ujjwal M. Mahajan,^{1,2} Bettina Oehrlé,^{1,2} Simon Sirtl,^{1,2} Ahmed Alnatsha,^{1,2} Elisabetta Goni,^{1,2} Ivonne Regel,^{1,2} Georg Beyer,^{1,2} Marlies Vornhülz,^{1,2} Jakob Vielhauer,^{1,2} Ansgar Chromik,³ Markus Bahra,⁴ Fritz Klein,⁵ Waldemar Uhl,⁶ Tim Fahlbusch,⁶ Marius Distler,⁷ Jürgen Weitz,⁷ Robert Grützmann,^{8,9} Christian Pilarsky,^{8,9} Frank Ulrich Weiss,¹⁰ M. Gordian Adam,^{11,12} John P. Neoptolemos,¹³ Holger Kalthoff,¹⁴ Roland Rad,^{2,15} Nicole Christiansen,^{11,16} Bianca Bethan,¹¹ Beate Kamlage,¹¹ Markus M. Lerch,^{2,10,17} and Julia Mayerle^{1,2}

¹Department of Medicine II, University Hospital, Ludwig Maximilian University of Munich, Munich; ²Bavarian Centre for Cancer Research (Bayerisches Zentrum für Krebsforschung), Munich; ³Department of General and Visceral Surgery, Asklepios Klinikum Hamburg, Hamburg; ⁴Zentrum für Onkologische Oberbauchchirurgie und Robotik, Krankenhaus Waldfriede, Berlin; ⁵Department of General, Visceral and Transplantation Surgery, Charité, Campus Virchow Klinikum, Berlin; ⁶Department of General and Visceral Surgery, Katholisches Klinikum Bochum, Bochum; ⁷Department for Visceral, Thoracic and Vascular Surgery, University Hospital, Technische Universität Dresden, Dresden; ⁸Department of Surgery, Erlangen University Hospital, Erlangen; ⁹Bavarian Centre for Cancer Research (Bayerisches Zentrum für Krebsforschung), Erlangen; ¹⁰Department of Medicine A, University Medicine Greifswald, Greifswald; ¹¹Metanomics Health GmbH, Berlin, Germany; ¹²biocrates life sciences ag, Innsbruck, Austria; ¹³Department of General, Visceral and Transplantation Surgery, University of Heidelberg, Heidelberg; ¹⁴Section for Molecular Oncology, Institut für Experimentale Krebsforschung (IET), Universitätsklinikum Schleswig-Holstein, Kiel; ¹⁵Institute of Molecular Oncology and Functional Genomics, TUM School of Medicine and Center for Translational Cancer Research (TranslaTUM), Technische Universität München, Munich; ¹⁶TrinamiX GmbH, Ludwigshafen am Rhein, Rheinland-Pfalz; and ¹⁷Ludwig Maximilian University Klinikum, Munich, Germany



BACKGROUND & AIMS: Pancreatic ductal adenocarcinoma (PDAC) is a highly lethal malignancy requiring efficient detection when the primary tumor is still resectable. We previously developed the MxPancreasScore comprising 9 analytes and serum carbohydrate antigen 19-9 (CA19-9), achieving an accuracy of 90.6%. The necessity for 5 different analytical platforms and multiple analytical runs, however, hindered clinical applicability. We therefore aimed to develop a simpler single-analytical run, single-platform diagnostic signature. **METHODS:** We evaluated 941 patients (PDAC, 356; chronic pancreatitis [CP], 304; nonpancreatic disease, 281) in 3

multicenter independent tests, and identification (ID) and validation cohort 1 (VD1) and 2 (VD2) were evaluated. Targeted quantitative plasma metabolite analysis was performed on a liquid chromatography–tandem mass spectrometry platform. A machine learning-aided algorithm identified an improved (i-Metabolic) and minimalistic metabolic (m-Metabolic) signatures, and compared them for performance. **RESULTS:** The i-Metabolic Signature, (12 analytes plus CA19-9) distinguished PDAC from CP with area under the curve (95% confidence interval) of 97.2% (97.1%–97.3%), 93.5% (93.4%–93.7%), and 92.2% (92.1%–92.3%) in the ID, VD1, and VD2

cohorts, respectively. In the VD2 cohort, the m-Metabolic signature (4 analytes plus CA19-9) discriminated PDAC from CP with a sensitivity of 77.3% and specificity of 89.6%, with an overall accuracy of 82.4%. For the subset of 45 patients with PDAC with resectable stages IA-IIB tumors, the sensitivity, specificity, and accuracy were 73.2%, 89.6%, and 82.7%, respectively; for those with detectable CA19-9 >2 U/mL, 81.6%, 88.7%, and 84.5%, respectively; and for those with CA19-9 <37 U/mL, 39.7%, 94.1%, and 76.3%, respectively. **CONCLUSIONS:** The single-platform, single-run, m-Metabolic signature of just 4 metabolites used in combination with serum CA19-9 levels is an innovative accurate diagnostic tool for PDAC at the time of clinical presentation, warranting further large-scale evaluation.

Keywords: Metabolic Signature; Pancreatic Cancer; CA19-9; Chronic Pancreatitis; Diagnostic Signature.

Pancreatic ductal adenocarcinoma (PDAC) is a highly lethal malignancy with 5-year relative survival rates of only 11% for all stages. PDAC incidence is rising by ~1% per year and now in the United States ranks as the third commonest cause of cancer death.¹ The best results are achieved with surgical resection and adjuvant chemotherapy, with 5-year survival rates of 30% to 50%, but most patients present with locally advanced unresectable disease or metastases, or both.^{2,3} In symptomatic patients, the diagnosis is often delayed because of the difficulty in discriminating PDAC from benign pancreatic diseases, notably chronic pancreatitis (CP), which may also be associated with an increased risk of PDAC.⁴⁻⁸

Background inflammatory changes can mask underlying malignancy and reduce the sensitivity and accuracy of even the most accurate imaging method, such as endoscopic ultrasound and ultrasound-guided fine-needle aspiration.⁹ Establishing a cost-effective biomarker with high specificity and sensitivity could significantly improve the treatment and survival in these patients.^{10,11} We recently developed a metabolic signature (MxPancreasScore), which used in conjunction with carbohydrate antigen 19-9 (CA19-9), distinguished PDAC from CP with clinically relevant higher diagnostic accuracy than CA19-9 alone.¹⁰ The MxPancreasScore, however, lacks clinical generalizability because it requires multiple analytical platforms and multiple analytical runs using liquid chromatography/mass spectrometry, also resulting in reduced cost-effectiveness.¹²

We therefore aimed to improve and optimize the MxPancreasScore to reduce analytical hurdles. To derive an effective signature with the minimal number of analytes, a machine learning (ML)-based feature reduction strategy was used. We tested the performance of the new signature(s) prospectively in an independent multicenter case-control study that compared patients with PDAC with those with CP, as well as with patients with nonpancreatic diseases (NPC), such as liver cirrhosis and acute cholangitis, and otherwise healthy individuals due to undergo operations for benign conditions, including thyroidectomy, hernia

WHAT YOU NEED TO KNOW

BACKGROUND AND CONTEXT

Pancreatic cancer is a highly lethal malignancy, in part due to late-stage presentation, necessitating efficient and accurate detection when the primary tumor is still resectable in order to contribute to improved outcomes.

NEW FINDINGS

Investigating 941 patients with and without pancreatic cancer, split into test and validation cohorts, we demonstrate that the m-Metabolic signature (comprising only 4 analytes plus carbohydrate antigen 19-9) identifies pancreatic cancer with a high overall accuracy.

LIMITATIONS

There were relatively small numbers of patients with very early-stage cancers and a predominance of patients with a Caucasian background.

IMPACT

The m-Metabolic signature of just 4 analytes used in combination with serum carbohydrate antigen 19-9 levels is an innovative diagnostic tool with a potential major impact on the management of pancreatic cancer.

repair, and elective cholecystectomy, in accordance with the Early Detection Research Network guidelines.^{13,14}

Materials and Methods

Study End Points

The primary end point of the study was discrimination of PDAC from CP in plasma samples. The secondary end points were discrimination of resectable PDAC from CP and discrimination of PDAC from NPC controls.

Patient Recruitment and Sample Collection

The study recruited 941 patients with pathologically confirmed PDAC or CP and patients with NPC due for elective operations in 3 independent multicenter prospective cohorts according to the Standards for the Reporting of Diagnostic Accuracy Studies (STARD) guidelines.¹⁵ These were the identification cohort (ID, October 2002–November 2011), validation cohort 1 (VD1, January 2009–August 2013), and validation cohort 2 (VD2, September 2013–September 2015). The ID and VD1 cohorts were described previously.¹⁰ All patients gave their written informed consent, and the local Ethics Review

Abbreviations used in this paper: automl, automated machine learning; AUC, area under the curve; BMI, body mass index; CA19-9, carbohydrate antigen 19-9; CI, confidence interval; CP, chronic pancreatitis; ID, identification cohort; LC-MS/MS, liquid chromatography-tandem mass spectrometry; ML, machine learning; NPC, nonpancreatic disease; NPV, negative predictive value; PDAC, pancreatic ductal adenocarcinoma; VD1, validation cohort 1; VD2, validation cohort 2.

Most current article

© 2022 The Author(s). Published by Elsevier Inc. on behalf of the AGA Institute. This is an open access article under the CC BY-NC-ND license (<http://creativecommons.org/licenses/by-nc-nd/4.0/>).

0016-5085

<https://doi.org/10.1053/j.gastro.2022.07.047>

Boards approved the protocol at all participating centers (Berlin, EA4/085/13; Bochum, 4452-12; Dresden, EK49022014).

The analyses were performed retrospectively. Demographic, clinical, and pathologic variables are reported in Table 1. Before initiation of cancer treatment and after overnight fasting, blood samples were collected in EDTA tubes and processed for plasma isolation, as described previously.¹⁰ CA19-9 levels were determined at a centralized certified clinical laboratory with an upper limit of normal of 37 U/mL.

Validation Cohort 2 Power Calculations

For the VD2 study, power analysis was performed to estimate an adequate sample size based on representative metabolite profiling standard deviations that were determined in earlier studies. The primary aim of the study was to determine a

20% difference of analyte levels at a 5% significance level with a power of 72% to 99%. The analyte difference was defined as absolute or relative difference in concentrations of individual analytes. Power estimates were based on the *t* test statistic.

m-Metabolic Signature Substudies

To estimate the robustness of the m-Metabolic signature in clinical routine, 2 independent substudies were undertaken comprising in each 20 self-reported healthy subjects meeting the following inclusion criteria: age, 18 to 60 years; body mass index (BMI), 17.5 to 30.5 kg/m²; and 8- to 12-hour fasting before blood draw. Ethics approval was obtained under the protocol 011/1763. CA19-9 levels of these individuals were simulated between 0 and 37 U/mL, with 100 independent iterations to exclude bias. EDTA blood and plasma from the first group of 20 subjects (median age, 43 years; median BMI,

Table 1. Patient Characteristics and Distributions According to Project Phases

Variable	ID (n = 156)	VD1 (n = 235)	VD2 (n = 550)	Total (N = 941)
Center				
Berlin-Mitte	0 (0.0)	0 (0.0)	52 (9.5)	52 (5.5)
Berlin-Virchow	0 (0.0)	0 (0.0)	136 (24.7)	136 (14.5)
Bochum	0 (0.0)	0 (0.0)	205 (37.3)	205 (21.8)
Dresden	156 (100.0)	235 (100.0)	157 (28.5)	548 (58.2)
Sex				
Female	46 (29.5)	96 (40.9)	183 (33.3)	325 (34.5)
Male	110 (70.5)	139 (59.1)	367 (66.7)	616 (65.5)
Age, y				
Mean (SD)	60.0 (11.8)	60.9 (13.4)	58.5 (13.8)	59.3 (13.4)
Range	25.0–82.0	20.0–88.0	22.0–90.0	20.0–90.0
BMI, kg/m²				
Missing	0	1	0	1
Mean (SD)	23.9 (3.4)	25.1 (4.8)	25.3 (4.6)	25.0 (4.5)
Range	13.9–34.1	14.5–49.9	15.7–48.9	13.9–49.9
CA19-9, U/mL				
Mean (SD)	409.1 (1384.5)	749.4 (6553.3)	400.9 (2365.8)	489.3 (3781.3)
Range	0.3–11,622.0	0.6–98,060.0	0.6–50,000.0	0.3–98,060.0
Diabetic status				
Missing	1	7	9	17
No	85 (54.8)	140 (61.4)	405 (74.9)	630 (68.2)
Yes	70 (45.2)	88 (38.6)	136 (25.1)	294 (31.8)
UICC classification^a				
Missing or N.A. ^b	79	158	349	586
IA	0 (0.0)	1 (1.3)	4 (2.0)	5 (1.4)
IB	2 (2.6)	0 (0.0)	2 (1.0)	4 (1.1)
IIA	16 (20.8)	11 (14.3)	33 (16.4)	60 (16.9)
IIB	36 (46.8)	28 (36.4)	64 (31.8)	128 (36.1)
III	18 (23.4)	24 (31.2)	30 (14.9)	72 (20.3)
IV	5 (6.5)	13 (16.9)	68 (33.8)	86 (24.2)
Tumor stage				
Missing or N.A. ^b	97	235	352	684
T1	0 (0.0)	0	6 (3.0)	6 (2.3)
T2	4 (6.8)	0	5 (2.5)	9 (3.5)
T3	55 (93.2)	0	99 (50.0)	154 (59.9)
T4	0 (0.0)	0	10 (5.1)	10 (3.9)
Inoperable	0 (0.0)	0	78 (39.4)	78 (30.4)

Table 1. Continued

Variable	ID (n = 156)	VD1 (n = 235)	VD2 (n = 550)	Total (N = 941)
Lymph node invasion				
Missing or N.A. ^b	97	235	408	740
N0	19 (32.2)	0	44 (31.0)	63 (31.3)
N1	40 (67.8)	0	77 (54.2)	117 (58.2)
X	0 (0.0)	0	21 (14.8)	21 (10.4)
Metastases				
Missing or N.A. ^b	97	235	351	683
M0	54 (91.5)	0	125 (62.8)	179 (69.4)
M1	3 (5.1)	0	67 (33.7)	70 (27.1)
X	2 (3.4)	0	7 (3.5)	9 (3.5)
Tumor grading				
Missing or N.A. ^b	107	235	360	702
G1	0 (0.0)	0	6 (3.2)	6 (2.5)
G2	27 (55.1)	0	69 (36.3)	96 (40.2)
G3	22 (44.9)	0	69 (36.3)	91 (38.1)
G4	0 (0.0)	0	3 (1.6)	3 (1.3)
X	0 (0.0)	0	43 (22.6)	43 (18.0)
Diagnosis				
CP	79 (50.6)	79 (33.6)	144 (26.2)	302 (32.1)
NPC	0 (0.0)	79 (33.6)	204 (37.1)	283 (30.1)
PDAC	77 (49.4)	77 (32.8)	202 (36.7)	356 (37.8)

NOTE. Data are presented as n (%), unless indicated otherwise.

N.A., not applicable; SD, standard deviation; UICC, Union for International Cancer Council.

^aUICC TNM Classification, 6th Edition.

^bN.A. for benign diseases.

23 kg/m²) were analyzed to assess the effect of different blood collection tubes, short-term room temperature storage, and storage at -20°C. To understand the influence of fasting or non-fasting status on metabolic profiles, a second group of 20 subjects (median age, 38 years; median BMI, 24 kg/m²) EDTA plasma samples were collected after overnight fasting, 1.5 to 2.5 hours after breakfast, and 1.5 to 2.5 hours after a light lunch. The potential effect of common comedications was analyzed by using previously collected multicenter samples obtained from the VD2 cohort.

Plasma Analyte Analysis

Targeted quantitative plasma analyte analysis was performed on a liquid chromatography-tandem mass spectrometry (LC-MS/MS) platform. Human plasma samples were prepared and were analyzed by LC-MS/MS as follows: 20 μL human plasma was mixed with 100 μL internal standard mixture (alanine d4: 12.24 μg/mL and ceramide [d18:1,C17:0]: 0.154 μg/mL were dissolved in dimethyl sulfoxide, methanol, dichloromethane, and water [in a ratio 12.3:2.2:1.1:1, v/v/v/v]), and 700 μL extraction solvent containing methanol and dichloromethane in a ratio of 2:1 (v/v). After the samples were thoroughly mixed at 20°C for 5 minutes, the precipitated proteins were removed by centrifugation for 10 minutes. Then, 150 μL of the liquid supernatant was transferred to an appropriate glass vial for further derivatization with dansyl chloride, which allows the dansylation of primary and secondary amine groups. For this purpose, 25 μL of 0.2 mol/L sodium bicarbonate buffer (dissolved in water), 25 μL of 4 mg/mL dansyl chloride solution

(dissolved in acetonitrile), and 50 μL dimethyl sulfoxide were added. The dansylation was performed under constant mixing at 35°C for 150 minutes.

The obtained reaction mixtures were analyzed by LC-MS/MS. The LC-MS/MS systems consisted of an Agilent 1100 LC system (Agilent Technologies, Waldbronn, Germany) coupled with an API 4000 MS (ABSCIEX, Toronto, ON, Canada). High-performance LC analysis was performed on commercially available reversed-phase separation columns with C18 stationary phases (Phenomenex Ascentis Express C18, 2.7 μm, 50 × 2.1 mm). Up to 2 μL of the above-mentioned so-obtained reaction mixture was injected and separated by gradient elution using a mixture of solvents consisting of methanol, water, formic acid, 2-propanol, and 2-methoxy-2-methylpropane at a flow rate of 600 μL/min (starting from 0% solvent B to 100% solvent B in 7 minutes): Solvent A: 400 g methanol, 400 g water, 1 g formic acid; solvent B: 400 g 2-methoxy-2-methylpropane, 200 g 2-propanol, 100 g methanol, and 1 g formic acid.

MS was performed by electrospray ionization in positive ion mode using multiple reaction monitoring. Electrospray ionization detected sphingomyelins with equal numbers of carbons and double bonds, and these isobaric species were not separated chromatographically. Quantitative evaluations of all metabolites with commercially available quantification standards were achieved by external calibration in delipidized plasma (ceramide [d18:1,C17:0] was used as the external standard for sphingomyelins, and ceramide [d4-alanine] was used as the external standard for amino acids and ethanolamines).

Imputation, Scaling, and Predictive Modeling

All analyte profiling data were \log_{10} -transformed to achieve an approximately normal distribution. The \log_{10} -transformed, autoscaled, and median imputed ratios were used for further analysis.

The elastic-net generalized linear regression modeling, a linear combination of L_1/L_2 regularization, was used for building the predictions to stratify patients with PDAC from CP and NPC, based on metabolic profiles in the ID cohort obtaining a predictive model (i-Metabolic signature). The penalties were determined for both L_1 and L_2 norms using a cross-validation grid search with the R glmnet package (R Foundation for Statistical Computing, Vienna, Austria). Optimal cutoff for the i-Metabolic signature was analyzed by a cost-sensitive approach using the cost function¹⁶ on the VD1 data set, with approximation of cost of false positive as 1, whereas the cost of false negative was set as 2. Performance statistics of the i-Metabolic signature at optimal cutoff was analyzed using 10-fold cross-validation and bootstrapping for the VD1 and VD2 cohort.

To optimize the number of variables without compromising the performance, the base ML model was constructed using the H2O.ai platform (<https://h2o.ai/>) automatically selecting (with h2o.automl) the best suitable ML method on the ID cohort. To save computational time, the selection of methods was limited to generalized linear models, random forests, and gradient-boosting machines. The parameters of each method were optimized by using an internal 10-fold cross-validation on the ID cohort. The optimal method was then applied to the VD1 cohort to assess final performance and optimal cutoff using the F1 score.

In each loop, the best performing predictive model was identified from all obtained predictive models using the performance measure logloss. Variables associated with the base ML model were selected according to their scaled importance >0.05 to obtain an iterated ML model that was based on a reduced set of variables ($n = 11$). To obtain the best performing predictive model based on a minimalistic set of variables, variables of the iterative ML model were ranked according to their scaled importance. Leaving out the lowest-ranking variable, a new predictive model was trained on the ID cohort, and its performance evaluated on the VD1 cohort. Again, the lowest-ranking variable on the remaining set of variables was removed and a new predictive model was generated and tested in the same way. This procedure was repeated until no variable remained. Out of these predictive models, the m-Metabolic signature was selected, which best matched the tradeoff between good performance and minimal set of variables. Performance statistics of the i-Metabolic signature at optimal cutoff were analyzed using 10-fold cross-validation on VD1 and VD2 cohort.

Interference Testing

With the aim to optimize the m-Metabolic signature, the effect of interference was tested with the Assurance Interference kit (Sun Diagnostics, New Gloucester, ME) according to the manufacturer's instructions. Interferents included hemolysate, conjugated and unconjugated bilirubin, total proteins, and triglyceride-rich lipoproteins. For the interference analysis, 2 different pooled plasma samples were used (pool 1 and pool 2). Pools were corrected for baseline interferent levels and spiked by interferent solutions and subjected to metabolic profiling, as

described above. Relative fold-changes of obtained metabolites were quantified against naive high and low pools, respectively. Furthermore, the interferent solution was spiked in saline solution and subjected to metabolic profiling to understand influence of the interferent on metabolic profiling. The total allowable error (TAE) was calculated according to the EP07 guidelines (Clinical and Laboratory Standards Institute), separately for each metabolite and for each interferent: $TAE = \text{Experimentally determined bias} \pm 3 \text{ SD}$, with SD indicating the standard deviation. From the total allowable error, the acceptable limit (D_{\min} and D_{\max}) was calculated. If the lower confidence interval (CI) limit of the fold-change was lower than D_{\min} or the upper CI limit of the fold-change was above the D_{\max} , the difference was considered clinically significant.¹⁷

Statistical Analyses

All data processing, modeling, and assessment of performances was performed using R 4.0.4 software (2021-02-15, "Lost Library Book") and visualized in RStudio 1.3.959 (Boston, MA). No unique algorithm was developed for this study. All data, R scripts, or functions used are outlined under <https://github.com/mayerlelab/assayDevelopment.git>. Comparative receiver operating characteristics curve testing was performed using bootstrap testing for a difference in the area under the curve (AUC) of all receiver operating characteristics curves. For preanalytical and comedication studies, Wilcoxon's rank sum test, followed by Bonferroni's correction, were performed for comparison with baseline. P values of $<.05$ were considered statistically significant if appropriate for the tests used.

Results

Patient Characteristics

The characteristics of the study participants for each cohort are listed in Table 1 and Figure 1A. There were 356 patients with pathologically confirmed PDAC recruited in 3 independent multicenter prospective cohorts. In the ID cohort, 79 patients with CP were recruited, and in the VD1 and VD2 cohorts, 79 and 144 patients with CP, balanced for age and sex, were recruited, respectively. Additionally, in the VD1 and VD2 cohorts, 77 and 204 patients with NPC or liver diseases were enrolled. Only EDTA plasma metabolite profiling from all of the enrolled patients was considered for the analysis. A cumulative PDAC incidence of 1.95% in patients diagnosed with CP^{8,10} was set for the analysis of model performance.

Improvement and Independent Validation of Metabolic Signatures

Previously, we delineated the MxPancreasScore that could distinguish between PDAC and CP with greater accuracy than preexisting conventional tumor markers as well as microRNA panels.¹⁰ Although efficient, the MxPancreasScore required 5 different analytical platforms and multiple analytics runs, thus impeding clinical applicability and increasing diagnostic test expenditure. Any widely applicable PDAC blood diagnostic test should approach the screening level at €400 assuming a quality-adjusted life-year cost of €13,500.¹⁸ Taking these criteria into

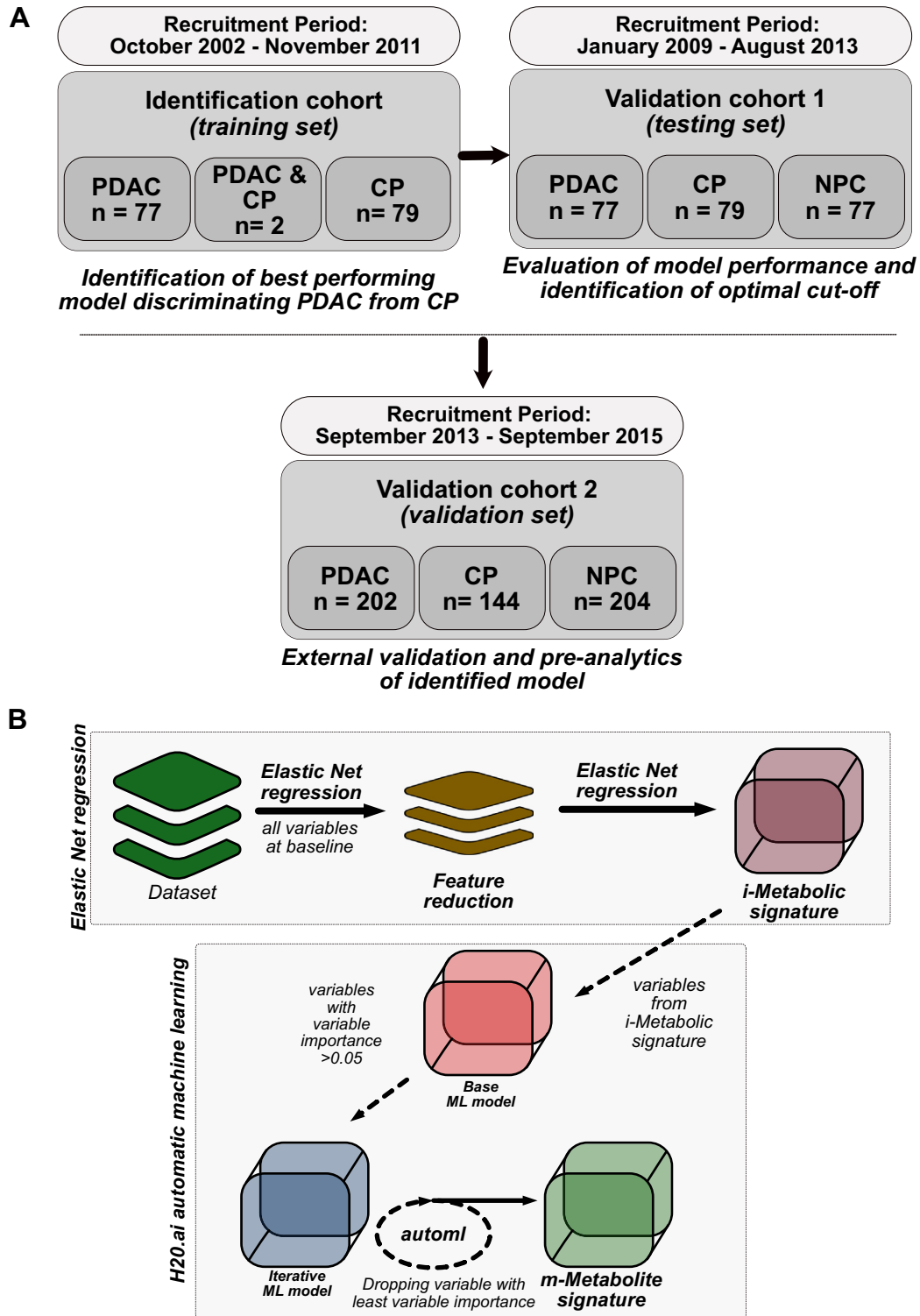


Figure 1. Consolidated Standards of Reporting Trials diagram of patients recruited for metabolome analysis and downstream identification of our improved metabolic biomarker signature. (A) All patients were recruited prospectively in three different independent trials (ID cohort, VD1, and VD2). The best performing model was identified using the ID cohort and tested for its efficiency in the VD1 cohort. Patients for the VD2 cohort were recruited independently as a second independent cohort to evaluate model performance. (B) Schematic workflow illustrates the identification of metabolic biomarker signatures using elastic net regression (i-Metabolic signature) and using automl for the iterative reduction of variables to identify the m-Metabolic signature.

consideration we only considered those analytes that could be measured on a single analytical platform in 1 run to be included in the metabolic signature. The improved metabolic signature (i-Metabolic signature), using feature reduction and elastic net regression, consisted of 12 analytes plus CA19-9 (Figure 1B and Figure 2A).

The i-Metabolic signature distinguished PDAC from CP with an AUC of 0.972 (95% CI 0.971–0.973), significantly outperforming CA19-9 alone with an AUC of 0.893 (95% CI, 0.891–0.895, $P = .003$) in the ID cohort (Figure 2B). The optimum cutoff for the i-Metabolic signature was set to ≥ 0.572 based on the implementation of the cost functions for the VD1 cohort. The cutoff was then transferred to all cohorts, and the diagnostic performance was evaluated. This revealed a sensitivity of 90.8% (95% CI, 90.6%–91.0%) at a specificity of 87.7% (95% CI, 87.5%–87.9%) for the i-Metabolic signature, whereas for CA19-9 alone, a sensitivity of 75.1% (95% CI, 74.8%–75.4%) at a specificity of 75.9% (95% CI, 75.6%–76.2%; $P < .001$) was demonstrated for the VD1 cohort (Figure 2B).

Validation of the Clinical Performance of the i-Metabolic Signature in the Validation 2 Cohort

In the VD2 study, the i-Metabolic signature distinguished between PDAC and CP with an AUC of 0.922 (95% CI, 0.921–0.923), at a specificity of 92.2% (95% CI, 92.1%–92.3%), and a sensitivity of 79.6% (95% CI, 79.4%–79.8%), resulting in a negative predictive value (NPV) of 99.5% (95% CI, 99.5%–99.5%), when assuming a cumulative incidence of 1.95% of PDAC in the CP population (Figure 2B and Table 2). The diagnostic accuracy was calculated with 86.3% (95% CI, 86.2%–86.4%). In the VD2 cohort, for CA19-9 alone, an AUC of 0.828 (95% CI, 0.826–0.829; $P < .001$) was detected. Furthermore, the i-Metabolic signature detected resectable PDAC (82 of 104) with an accuracy of 85.3% (95% CI, 85.2%–85.5%). Of note, the i-Metabolic signature demonstrated a diagnostic accuracy of 89.9% (95% CI, 89.7%–90.0%) in a subset analysis of patients with CA19-9 levels below the clinical cutoff of <37 U/mL (Table 2 and Supplementary Table 1).

When the i-Metabolic signature was analyzed for the discriminatory strength between PDAC and the different control cohorts of NPC or CP, no significant difference between CP and NPC was observed (Figure 2C). Comparison of the i-Metabolic signature with CA19-9 alone (cutoff, 37 U/mL¹⁹) revealed that using the i-Metabolic signature would have diagnosed an additional 15.3% of patients with PDAC (marked in orange) and would have correctly identified 11.8% patients with CP, who would have been misdiagnosed as patients with PDAC (marked in green) using CA19-9 alone in the VD2 cohort (Figure 2D).

Because CA19-9 is an important component of the i-Metabolic signature, we addressed the question of performance status of the i-Metabolic signature in CA19-9 nonsecretory patients. CA19-9 levels <2 U/mL were considered likely to be patients negative for Lewis antigen a and b, and thus may lead to false-negative results.²⁰ We

observed that the i-Metabolic signature distinguished patients with PDAC from patients with CP with an AUC of 0.938 (95% CI, 0.937–0.939) in Lewis-positive patients with ≥ 2 U/mL CA19-9 levels. The i-Metabolic signature without CA19-9 in Lewis-negative patients with CA19-9 levels <2 U/mL stratified PDAC from CP with an AUC of 0.978 (95% CI, 0.977–0.980), with a specificity of 85.4% (95% CI, 84.8%–86.1%) at a sensitivity of 100% with an optimal cutoff of ≥ 0.362 , resulting in accuracy of 91.4% (Figure 3A).

Optimization of the i-Metabolic Signature

To further reduce the analyte number of the i-Metabolic signature to ease assay generation and to reduce costs, and so improve generalizability, we compiled an automatic ML-aided (automl) model incorporating all the analytes from the i-Metabolic signature. The workflow for h2o-aided automl is graphically represented in Figure 1B. We compiled the base ML model by training it on the ID cohort. To further advance the base ML model generation, we focused on a smaller set of variables by iteratively reducing variables with variable importance of <0.05 , resulting in a reduction of variables with least importance. We obtained a minimalistic ML model (m-Metabolic signature) comprising 4 metabolites plus CA19-9 (Figure 3B). This signature successfully discriminated PDAC from controls with an AUC of 0.904 (95% CI, 0.901–0.908) in the VD2 cohort (Figure 3C, Table 2, and Supplementary Table 2). Hitherto, the optimal cutoff for the m-Metabolic signature was set to ≥ 0.676 based on the performance metric max-F1. On transfer of the cutoff to the VD2 cohort, the m-Metabolic signature exhibited an accuracy of 82.4% (95% CI, 82.0%–82.8%) at a sensitivity of 77.3% (95% CI, 76.5%–78.1%) and specificity of 89.6% (95% CI, 88.8%–90.4%), with an NPV of 99.5% (Table 3). Of note, all the metabolites in the m-Metabolic signature can be measured using a single platform in 1 analytical run and minimizing assay costs without compromising performance.

The m-Metabolic signature was then evaluated in the VD2 cohort with respect to our previously published MxPancreasScore.¹⁰ The MxPancreasScore discriminated PDAC from CP with an AUC of 0.908 (95% CI, 0.907–0.909), matching the performance of the m-Metabolic signature ($P = .827$) (Supplementary Figure 1A). For the m-Metabolic signature we detected a false-negative rate of 10.4% vs 17.3% (Supplementary Figure 1B) in the MxPancreasScore.

Subsequently, to further evaluate the performance of the m-Metabolic signature, we performed a subset analysis in Lewis-negative patients. In this the m-Metabolic signature distinguished patients with PDAC from patients with CP with an AUC of 0.924 (95% CI, 0.920–0.927) in “Lewis positive” patients, whereas the m-Metabolic signature without CA19-9 in Lewis-negative patients displayed an AUC of 0.805 (95% CI, 0.79–0.818) and a diagnostic accuracy of 74.5% (95% CI, 72.3%–76.7%). Thus, the i-Metabolic signature without CA19-9 did not lose accuracy (Supplementary Figure 2). To enhance readability of the different metabolic signatures presented here in Lewis-negative patients, we delineated a decision tree for the

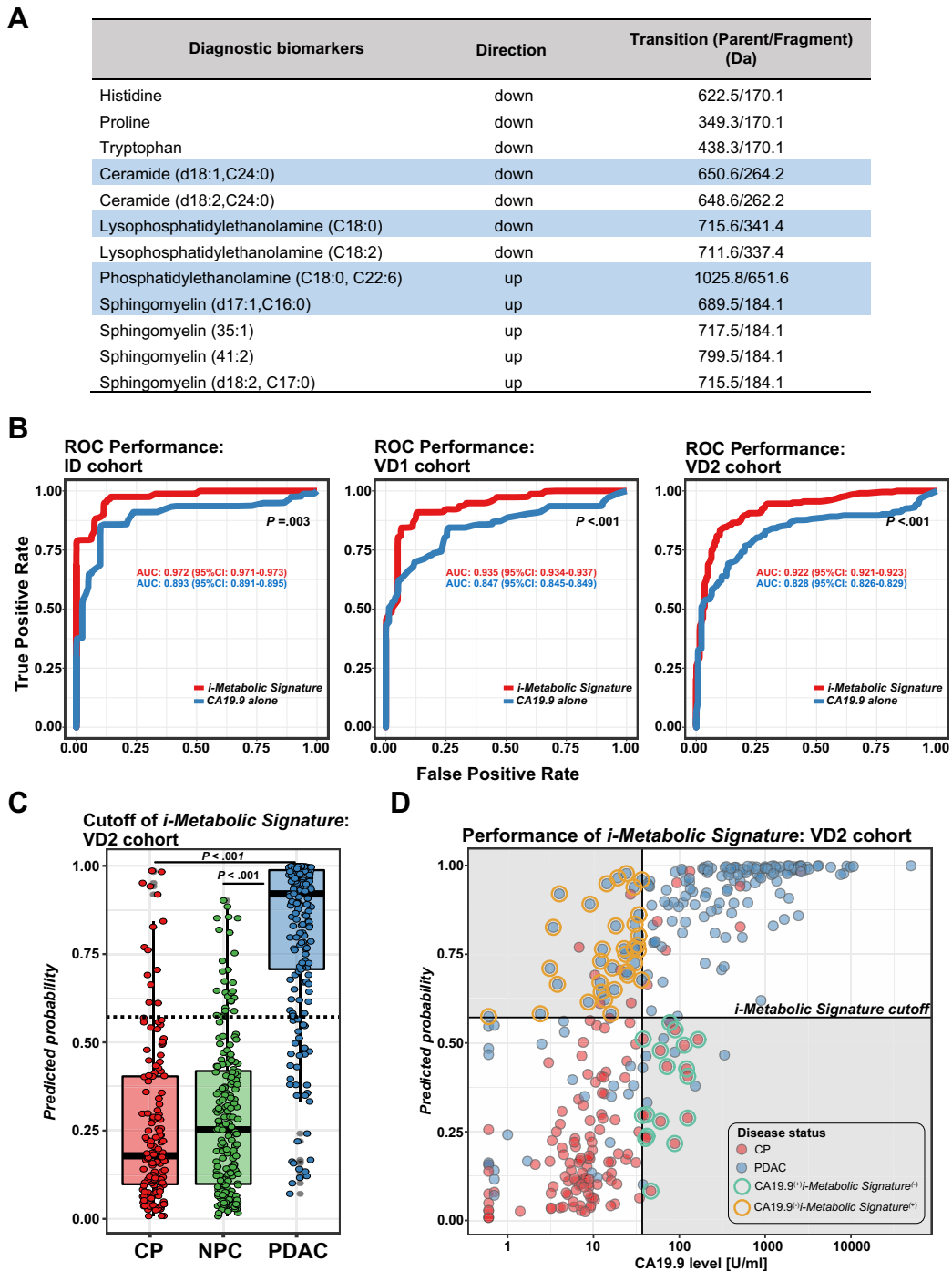


Figure 2. Identification of improved metabolic biomarkers signature (*i*-Metabolic signature). (A) List of metabolites in the *i*-Metabolite signature. Direction refers to direction of fold-change of the respective metabolite in PDAC compared with NPC disease controls. Metabolites marked in blue are part of the m-Metabolic signature. (B) Comparative receiver operating characteristics (ROC) curves of *i*-Metabolic signature and CA19-9 levels in the ID, VD1, and VD2 cohorts. *P* values are reported for comparative ROC curves. (C) Box plot illustrates distribution of predictive score of the *i*-Metabolic signature in the VD2 cohort. The diagnostic cutoff of the *i*-Metabolic signature was set to ≥ 0.572 (horizontal dotted line). The horizontal line in the middle of each box indicates the median; the top and bottom borders of the box mark the 75th and 25th percentiles, respectively, and the vertical lines mark the minimum and maximum of all the data. Wilcoxon's rank sum test in the box plot. (D) Scatter plot demonstrates performance of the *i*-Metabolic signature. The y-axis depicts the predictive score of the *i*-Metabolic signature, whereas the x-axis represents CA19-9 levels. The orange encircled points denote subjects that benefit from the *i*-Metabolic signature in predicting PDAC, and green encircled points represent subjects that benefit from the *i*-Metabolic signature in prevention of misdiagnosis of PDAC.

Table 2. Performance Characteristics of the i-Metabolic Signature at the Cutoff of >0.572 and Carbohydrate Antigen 19-9 alone at the Cutoff of >37 U/mL for the Validation 2 Cohort

Variable (n = PDAC/ Total)	Model	AUC	Sensitivity	Specificity	PPV	NPV	Accuracy
All stages (n = 202/346)	i-Metabolic signature	0.922 (0.921–0.923)	0.796 (0.794–0.798)	0.922 (0.921–0.923)	0.178 (0.175–0.180)	0.995 (0.995–0.995)	0.863 (0.862–0.864)
	CA19-9 alone	0.828 (0.826–0.829)	0.673 (0.671–0.675)	0.851 (0.849–0.853)	0.085 (0.084–0.086)	0.992 (0.992–0.992)	0.760 (0.759–0.761)
Resectable tumors, stages IA-IIIB (n = 104/248)	i-Metabolic signature	0.909 (0.908–0.910)	0.853 (0.851–0.854)	0.854 (0.852–0.857)	0.110 (0.108–0.112)	0.996 (0.996–0.996)	0.853 (0.852–0.855)
	CA19-9 alone	0.832 (0.830–0.833)	0.777 (0.774–0.779)	0.738 (0.735–0.741)	0.057 (0.056–0.058)	0.994 (0.993–0.994)	0.762 (0.760–0.763)
Detectable CA19-9 (>2 U/mL) (n = 190/322)	i-Metabolic signature	0.938 (0.937–0.939)	0.843 (0.841–0.845)	0.922 (0.921–0.923)	0.186 (0.183–0.188)	0.996 (0.996–0.996)	0.887 (0.886–0.889)
	CA19-9 alone	0.866 (0.865–0.867)	0.698 (0.696–0.701)	0.852 (0.850–0.853)	0.088 (0.087–0.089)	0.993 (0.992–0.993)	0.779 (0.777–0.780)
CA19-9 (<37 U/mL) ^a (n = 58/177)	i-Metabolic signature	0.879 (0.877–0.882)	0.651 (0.645–0.657)	0.944 (0.942–0.945)	0.204 (0.200–0.209)	0.992 (0.992–0.992)	0.899 (0.897–0.900)

NOTE. Data are presented with the 95% CI.

PPV, positive predictive value.

^aCA19-9 alone is not applicable for CA19-9 <37 U/mL class prediction.

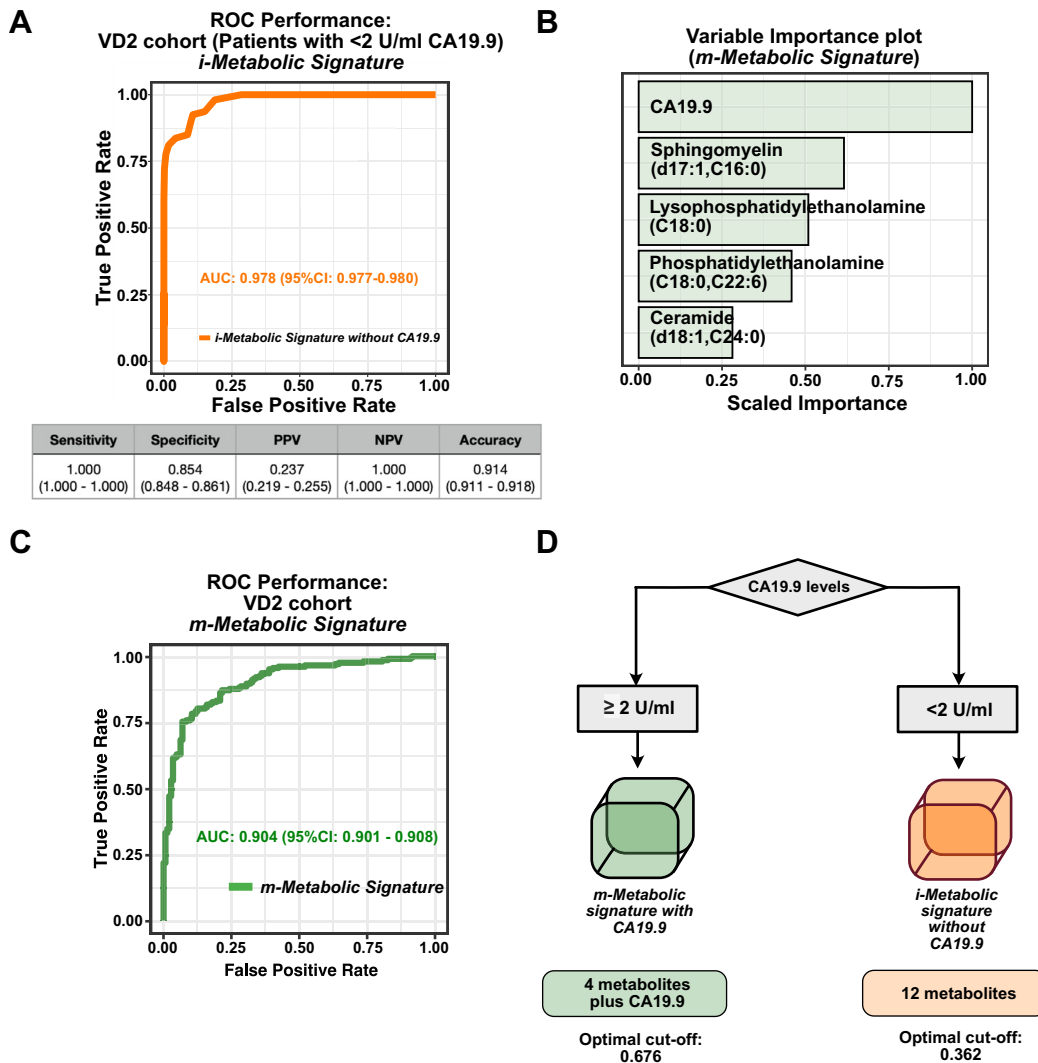


Figure 3. Optimization of *i*-Metabolic signature using automl. (A) Receiver operating characteristic (ROC) curves of the *i*-Metabolic signature without CA19-9 in patients with <2 U/mL CA19-9 in the VD2 cohort. PPV, positive predictive value. (B) Bar plot illustrates the ranks of the variables for the *m*-Metabolic signature by their scaled importance. (C) Comparative ROC curves of base ML model and *m*-Metabolic signature tested in the VD2 cohort. (D) Decision tree for the use of the *m*-Metabolic signature or *i*-Metabolic signature, with and without CA19-9, based on CA19-9 secretion status.

use the *m*-Metabolic and *i*-Metabolic signature based on CA19-9 levels (Figure 3D).

Evaluation of Preanalytical and Analytical Confounder Performance of the *m*-Metabolic Signature

To evaluate the preanalytical robustness, efficiency, and practical feasibility of the *m*-Metabolic signature for clinical routine use, the influence of different sample collection tube types, short-term storage at room temperature, storage at -20°C , influence of shipping, effect of hemolytic, lipemic, and icteric samples, influence of patients' fasting status, and influence of common comedications and comorbidities were tested.

The influence of different blood collection tubes, as outlined in Supplementary Figure 3A, was tested in blood samples of 20 self-reported healthy subjects in the morning

after overnight fasting. On metabolome analysis, we did not detect a significant deviation on the prediction probability in blood from different collection tube types (Supplementary Figure 3B). Because EDTA plasma is the preferred sample matrix for the *m*-Metabolic signature, room temperature storage for up to 48 hours was systematically studied, as shown in Supplementary Figure 4A. We did not detect significant changes in the prediction probability score upon incubation of plasma (Supplementary Figure 4B) or EDTA blood (Supplementary Figure 4C) over a period of 48 hours. To exclude the influence of short-term storage at -20°C , due to unavailability of ultralow temperature freezers in some clinical centers, performance of the *m*-Metabolic signature after storage over a 6-week period was evaluated. We did not detect a significant deviation in the prediction probability score of the *m*-Metabolic signature after short-term storage (Supplementary Figure 4D).

Table 3. Performance Characteristics of m-Metabolic Signature at the Cutoff of >0.676 for Validation 2 Cohort

Variable (n = PDAC/ Total)	AUC	Sensitivity	Specificity	PPV	NPV	Accuracy
All stages (n = 202/346)	0.904 (0.901–0.908)	0.773 (0.765–0.781)	0.896 (0.888–0.904)	0.130 (0.120–0.140)	0.995 (0.995–0.995)	0.824 (0.820–0.828)
Resectable tumors, stages IA–IIB (n = 104/248)	0.889 (0.885–0.893)	0.732 (0.720–0.743)	0.896 (0.887–0.905)	0.110 (0.108–0.112)	0.994 (0.993–0.995)	0.827 (0.822–0.832)
Detectable CA19-9 (>2 U/mL) (n = 190/322)	0.924 (0.920–0.927)	0.816 (0.808–0.824)	0.887 (0.878–0.895)	0.126 (0.117–0.136)	0.996 (0.996–0.996)	0.845 (0.841–0.849)
CA19-9 (<37 U/mL) (n = 58/177)	0.814 (0.806–0.822)	0.397 (0.378–0.415)	0.941 (0.935–0.946)	0.119 (0.108–0.130)	0.987 (0.987–0.987)	0.763 (0.757–0.768)

NOTE: Data are presented with the 95% CI. PPV, positive predictive value.

Because most patients with PDAC with a tumor mass in the head of the pancreas present with obstructive jaundice²¹ and hemolysis and jaundice and hyperlipemia are the most common causes of interference for accurate diagnostic prediction,²² we evaluated changes in metabolites associated with the m-Metabolic signature in hemolytic, icteric, lipemic, and high protein-containing samples. We spiked the 2 different human plasma pools with interferents. Although we did not observe a significant alteration in clinically relevant metabolites in hemolytic samples in both the high and the low pool, we observed significant alterations of complex lipid metabolites and fatty acids after spiking with triglycerides-containing lipoproteins in both plasma pools (Figure 4A). After correcting the interference by analytical methods, as expected, especially, lipoprotein spiking induces several fold-changes in the abundance of metabolites associated with the m-Metabolic signature (ceramide [d18:1,C24:0]), lysophosphatidylethanolamine [C18:0], phosphatidylethanolamine [C18:0,C22:6], and sphingomyelin [d17:1,C16:0]) (Figure 4B). We mapped out the influence of the fasting status on the m-Metabolic signature by evaluating the predictive potential of the m-Metabolic signature in 20 self-reported healthy subjects, as referred to in Figure 4C. We detected in those nonfasted subjects an ~50% decreased m-Metabolic signature probability prediction score, likely resulting in an increased number of false-negative subjects (Figure 4D).

According to the European Bioanalysis Forum recommendation, testing potential interference of comedications during assay development and validation is essential.²³ The potential effect of common comedications on the m-Metabolic signature was analyzed in the VD2 cohort. We analyzed 8 commonly used classes of drugs: proton pumps inhibitors, acetylsalicylic acid, pancreatic enzymes, and antihypertensive, antidiabetes, anticoagulant, lipid-lowering, and antigout drugs. Hitherto, we observed no relevant and statistically significant changes in the distribution of the prediction probability score of the m-Metabolic signature in discriminating PDAC from CP and NPC in users of these comedications (Figure 4E). In summary, the m-Metabolic signature in nonfasted patients may lead to a higher false-negative rate. With the exemption of lipemic plasma (triglycerides containing lipoproteins), the m-Metabolic signature showed robustness and stable performance under all conditions tested, rendering it a useful tool for clinical practice.

Discussion

To develop an assay for clinical routine use (Clinical Laboratory Improvement Amendments of 1988 [CLIA] application), we wanted to optimize and prospectively validate our previously described metabolic biomarker signature (MxPancreasScore),¹⁰ which distinguishes patients with PDAC from those with CP. The medical need of such an assay is high, because >90% of patients with PDAC die of the disease, making earlier detection of the disease critically important.²⁴ Diagnosis of PDAC is further impeded in the presence of CP. Our findings establish the value of a

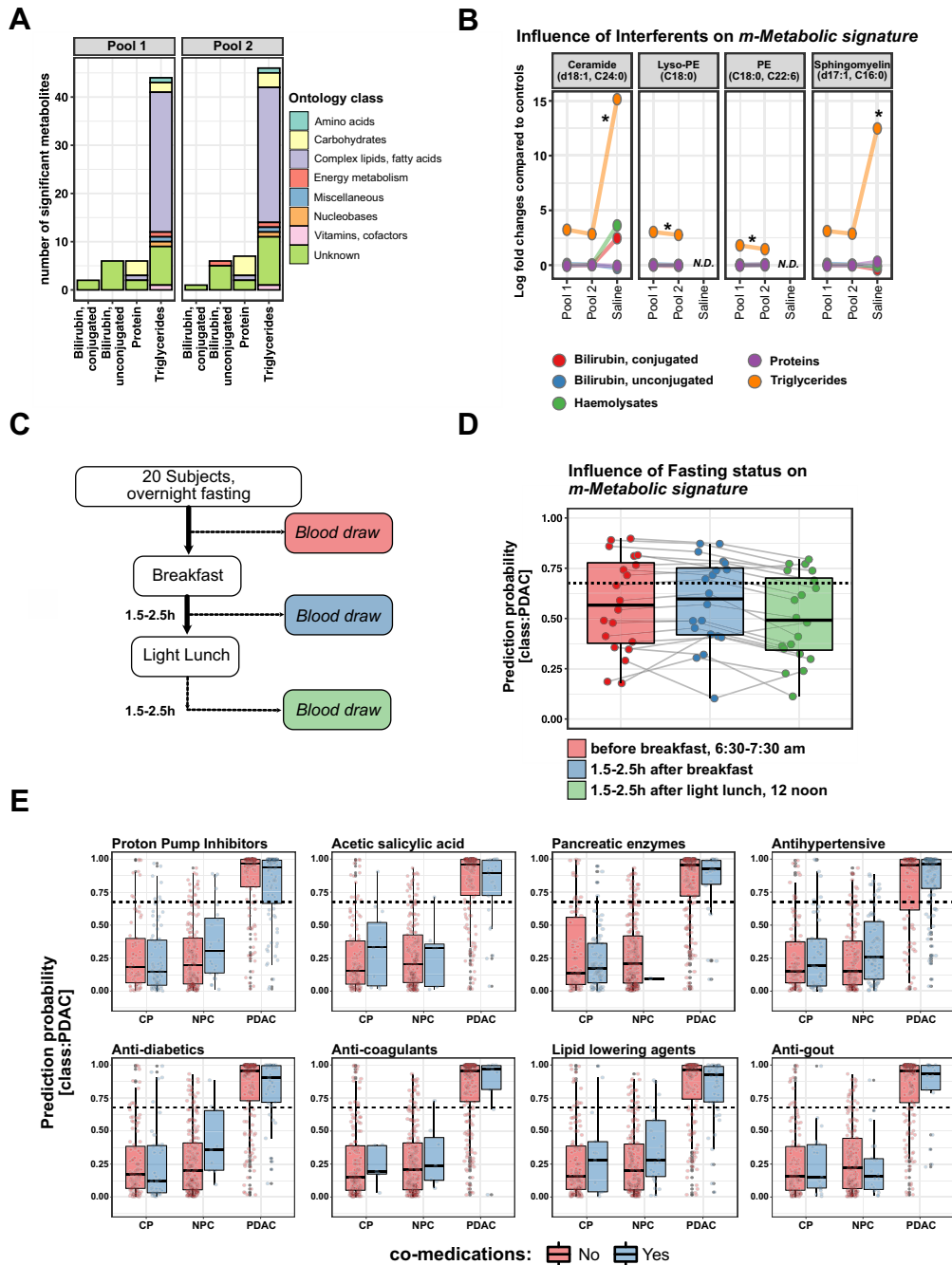


Figure 4. Robustness and optimization of the *m*-Metabolic signature for use in clinical routine. (A) *Bar plot* illustrates the number of clinically and statistically significant metabolites per metabolite ontology class after spiking of interferents in high concentrations (P0011) and in lower concentrations (P0012). Interferents spiked were hemolysates and conjugated and unconjugated bilirubin, proteins, and triglycerides. (B) Influence of spiking of interferents on the composition of the *m*-Metabolic signature. Triglycerides exert a considerable influence on the level of lipid metabolites in the *m*-Metabolite signature. N.D., not detected; PE, phosphatidylethanolamine. Wilcoxon’s rank sum test for comparative log fold-changes. (C) Schematics and study design testing the influence of fasting and nonfasting on the *m*-Metabolic signature. (D) *Box plot* illustrates the effect of nonfasting on the distribution of the prediction probability score of the *m*-Metabolic signature. The diagnostic cutoff of the *m*-Metabolic signature is based on the max F1 threshold and set to ≥ 0.676 (*horizontal dotted line*). The *connecting lines per dot* depict intrapatient variation. (E) *Box plots* depict the influence of comedications on the prediction probability of the *m*-Metabolic signature in discriminating PDAC from CP and NPC disease controls. Major comedications classes tested are proton pump inhibitors, acetylsalicylic acid, supplementary pancreatic enzymes, antihypertensive drugs, antidiabetes drugs, anticoagulants, lipid level-lowering drugs, and antigout medications. The diagnostic cutoff of the *m*-Metabolic signature is marked using a *horizontal dotted line*. The *horizontal line* in the middle of each *box* indicates the median; the *top and bottom borders* of the *box* mark the 75th and 25th percentiles, respectively, and the *vertical lines* mark the minimum and maximum of all the data. * $P < .05$ considered significant.

plasma-based m-Metabolic signature to discriminate PDAC from CP at the time of presentation. CA19-9 is the only blood-based tumor marker routinely used in the management of PDAC. However, limited sensitivity of CA19-9 in early-stage PDAC leads to false-negative results in patients, especially in subjects negative for Lewis antigen a and b. Suboptimal specificity in benign inflammatory pancreatic diseases and biliary obstruction limits its use for differential diagnoses.²⁵⁻²⁷

Previously, we delineated the MxPancreasScore, which distinguishes PDAC from CP with much greater accuracy than achieved by CA19-9 alone.¹⁰ Of 477 metabolites from 10 ontology classes, 29 metabolites were significantly altered between PDAC and CP in the serum and plasma of the training set. The Elastic Net algorithm identified 9 metabolites plus CA19-9 (MxPancreasScore), which discriminated PDAC from CP with an AUC of 0.96. The study was designed to exclude PDAC in patients with CP, with an emphasis placed on optimizing the NPV.^{10,28} The prototype MxPancreasScore necessitated 5 different analytical platforms and multiple runs, resulting in a relatively high diagnostic test expenditure.

In the present study, we optimized the metabolic signature using feature reduction and elastic net regression, resulting in 12 metabolites plus CA19-9 (i[*improved*]-Metabolic signature). The i-Metabolic signature in the present study was acquired by using a cost-sensitive approach.¹⁶ To this end, we found that with an optimal cutoff of ≥ 0.572 , the i-Metabolic signature discriminates patients with PDAC from those with CP with a specificity of 92.2% (NPV, 99.6%) and a sensitivity of 80% in an ID cohort. The i-Metabolic signature was built and selected on data from the ID cohort ($n = 158$) and VD1 cohort ($n = 233$), before the VD2 cohort ($n = 550$) was analyzed; therefore, our performance estimates were unbiased.

Variable and model performance optimization is an essential part of biomarker discovery.²⁹ To reduce overfitting and bias as well as to improve diagnostic measures and provide better informed, personalized patient-specific recommendations, we constructed h2o, an automatic ML platform driven to delineate and cross-validate the performance of the m(*inimalistic*)-Metabolic signature in an independent data set.³⁰ The optimal cutoff of the m-Metabolic signature was established, characterizing the performance of the m-Metabolic signature in the VD1 cohort by means of thresholding the F1 score³¹ with ≥ 0.676 as the cutoff. This cutoff was transferred to the VD2 cohort.

We recapitulated the performance of the i-Metabolic signature for the minimalistic ML-derived m-Metabolic signature, which now consists of only 4 metabolites plus CA19-9. The m-Metabolic signature distinguished patients with PDAC from patients with CP with a specificity of 90% (NPV, 99.5%) and a sensitivity of 78% in the ID cohort, matching its performance with the previously reported MxPancreasScore in the VD2 cohort. Of note, caution is needed because for any validation of diagnostic markers, the ultimate clinical usefulness of these biomarkers is influenced by the prevalence of the disease in the tested cohort.

We have therefore set up a prospective multicenter trial, Prospective Study on a Plasma Metabolome Multimarker

Panel MxP® PancreasScore for the Diagnosis of Pancreatic Cancer in Cohorts at Risk (META-PAC), recruiting patients with an undefined pancreatic mass on imaging in an enrichment design to establish the clinical use case (Deutsche Register Klinischer Studien registration #DRKS00010866). The recruitment goal of 1376 patients was reached in March 2020, and results are awaited after a follow-up period of 24 months.

The performance of the m-Metabolic signature was significantly better than CA19-9 alone in distinguishing PDAC from matched healthy subjects or CP, indicating potential relevance for the detection of early-stage PDAC. Taking into consideration the relative changes in metabolites associated with the m-Metabolic signature to controls and CP, the m-Metabolic signature might be suitable for the assessment of PDAC among patients with increased risk, such as a family history for PDAC,³² CP,³³ new-onset diabetes,^{34,35} and cystic lesions.³⁶

The response of the human plasma metabolome to preanalytical variation demands implementation of quality assurance and quality control to guarantee reproducible and reliable results.³⁷ Although the m-Metabolic signature showed robust performance, parameters that might jeopardize the quality and performance of the signature needed to be evaluated. Several important preanalytical factors that may seriously influence plasma metabolome profiles include mode of sample collection, collection time, processing delays, particularly at room temperature, repeated freeze/thaw cycles, and subsequent handling of the samples and transportation. The preanalytical challenges for metabolomics mainly lay in the stability of metabolites and cross-reactivity of metabolites during handling.^{38,39} Taking the differential availability of sample collection tubes and storage facilities in clinical routine into consideration, the m-Metabolic signature proved to be stable under different sample processing and transportation conditions.

Interference of hemolysis, jaundice, and lipemia poses important preanalytical hurdles in metabolome profiling.⁴⁰ Hemolysis is known to cause frequent problems in metabolic analysis because it leads to the release of proteins, enzymes, and metabolites in plasma.^{37,41} The presence of jaundice is one of the major limiting factors in the discrimination of PDAC from CP, because jaundice results in altered hepatic lipid metabolism and reduced biliary excretion of lipids and glycolipids, including CA19-9.⁴² Spiking with interferents revealed that although there is a change in global metabolic profiling in hemolytic and icteric samples, differences with respect to components of the m-Metabolic signature were not clinically relevant. Lipemic samples, considering the lipid-heavy m-Metabolic signature, can exert significant interference with detection and quantification of components of the m-Metabolite signature. As such as an expected finding, lipoprotein spiking exerted a considerable clinically significant bias on the lipid metabolites, and thus performance of the m-Metabolite signature in lipemic samples should be interpreted with caution.

Fasting status has been shown to contribute only marginally to the variability in the overall metabolome³⁹; still, it had a significant influence on lipid metabolites.⁴³

Because the m-Metabolic signature consists of lipid metabolites, fasting status was considered in the study design. We detected a significant increase in false-positive results in nonfasted patients using the m-Metabolic signature.

Growing apprehension for the interference of commonly used comedications on metabolite analytics of the m-Metabolite signature prompted us to study the impact of xenobiotics, including various medications and their metabolites, on metabolic homeostasis.⁴⁴ In our systematic study, we did not observe significant alterations in performance of the m-Metabolic signature in patients treated for comorbidities with comedications. Systematic studies such as ours are key for designing and validating diagnostic metabolic signatures to avoid systematic bias of metabolites concentration due to interferents.

An important strength of the present study was the large size of the 3 independent prospective data sets used in model optimization. Although promising PDAC plasma biomarkers have been previously reported,^{45–48} this is the first independent prospective sequential validation study where a previously identified metabolite-based signature¹⁰ was optimized for diagnostic and preanalytical performance and robustness in clinical routine. By applying rigorous statistical ML-based modeling, we were able to delineate a minimalistic predictor signature with statistically significantly improved performance over CA19-9 alone in distinguishing PDAC from CP in 3 independent cohorts. More importantly, even in sialyl Lewis-antigen nonsecreters, the performance of our i-Metabolic signature remained unchanged. A word of caution here is the inherent relatively low number of CA19-9-negative patients, and this finding needs to be validated in independent prospective cohorts of Lewis-negative patients.

A challenge for our present study is the validation of earlier PDAC detection with the metabolic signature. To demonstrate the utility of the m-Metabolic signature for PDAC screening, further validation of the m-Metabolic signature in a prediagnostic cohort of patients with a pancreatic mass lesion of unknown etiology at risk of PDAC is underway.

To the best of our knowledge, the only other diagnostic test as advanced as the m-Metabolic signature is the IMMray PanCan-d assay (Immunovia, Inc, Marlborough, MA), which was recently approved for CLIA use in the United States. Although efficient in screening high-risk patients, its performance for differential diagnoses has not been studied.⁴⁹ In addition, the medical need of identifying the ~1% of patients with newly diagnosed diabetes mellitus in a lean population aged >50 years has been recognized, and several important studies have been published.^{25,34,50–53} Furthermore, relevant prospective trials are underway.⁵⁴

Conclusions

Our findings demonstrate the utility of an optimized and validated m-Metabolic signature to discriminate PDAC from CP and from NPC subjects. The m-Metabolic signature encompasses plasma metabolites that can be analyzed in a single analytical setting and exhibits robust preanalytical performance in clinical routine. The m-Metabolic signature

keeps its performance in sialyl Lewis antigen nonsecreters. Further clinical studies are needed to prove its reliability, particularly in countries or regions with different ethnicity or resource settings.

Supplementary Material

Note: To access the supplementary material accompanying this article, visit the online version of *Gastroenterology* at www.gastrojournal.org, and at <https://doi.org/10.1053/j.gastro.2022.07.047>.

References

1. Siegel RL, Miller KD, Jemal A. Cancer statistics, 2018. *CA Cancer J Clin* 2018;68:7–30.
2. Kleeff J, Korc M, Apte M, et al. Pancreatic cancer. *Nat Rev Dis Primers* 2016;2:16022.
3. Neoptolemos JP, Palmer DH, Ghaneh P, et al. Comparison of adjuvant gemcitabine and capecitabine with gemcitabine monotherapy in patients with resected pancreatic cancer (ESPAC-4): a multicentre, open-label, randomised, phase 3 trial. *Lancet* 2017;389:1011–1024.
4. Conroy T, Desseigne F, Ychou M, et al. FOLFIRINOX versus gemcitabine for metastatic pancreatic cancer. *N Engl J Med* 2011;364:1817–1825.
5. Kennedy T, Preczewski L, Stocker SJ, et al. Incidence of benign inflammatory disease in patients undergoing Whipple procedure for clinically suspected carcinoma: a single-institution experience. *Am J Surg* 2006;191:437–441.
6. Schima W, Böhm G, Rösch CS, et al. Mass-forming pancreatitis versus pancreatic ductal adenocarcinoma: CT and MR imaging for differentiation. *Cancer Imaging* 2020;20:52.
7. Lowenfels AB, Maisonneuve P, Cavallini G, et al. Pancreatitis and the risk of pancreatic cancer. *N Engl J Med* 1993;328:1433–1437.
8. Vujasinovic M, Dugic A, Maisonneuve P, et al. Risk of developing pancreatic cancer in patients with chronic pancreatitis. *J Clin Med* 2020;9:3720.
9. Wolske KM, Ponnatapura J, Kolokythas O, et al. Chronic pancreatitis or pancreatic tumor? A problem-solving approach. *RadioGraphics* 2019;39:1965–1982.
10. Mayerle J, Kalthoff H, Reszka R, et al. Metabolic biomarker signature to differentiate pancreatic ductal adenocarcinoma from chronic pancreatitis. *Gut* 2018;67:128–137.
11. Hidalgo M. Pancreatic cancer. *N Engl J Med* 2010;362:1605–1617.
12. Wang S, Lifson MA, Inci F, et al. Advances in addressing technical challenges of point-of-care diagnostics in resource-limited settings. *Expert Rev Mol Diagn* 2016;16:449–459.
13. Pepe MS, Etzioni R, Feng Z, et al. Phases of biomarker development for early detection of cancer. *J Natl Cancer Inst* 2001;93:1054–1061.
14. Baker SG. Improving the biomarker pipeline to develop and evaluate cancer screening tests. *J Natl Cancer Inst* 2009;101:1116–1119.

15. Bossuyt PM, Reitsma JB, Bruns DE, et al. STARD 2015: an updated list of essential items for reporting diagnostic accuracy studies. *BMJ* 2015;351:h5527.
16. Skaltsa K, Jover L, Carrasco JL. Estimation of the diagnostic threshold accounting for decision costs and sampling uncertainty. *Biom J* 2010;52:676–697.
17. Guder WG, da Fonseca-Wollheim F, Heil W, et al. The haemolytic, icteric and lipemic sample recommendations regarding their recognition and prevention of clinically relevant interferences. Recommendations of the Working Group on Preanalytical Variables of the German Society for Clinical Chemistry and the German Society for Laboratory Medicine. *LaboratoriumsMedizin* 2000;24:357–364.
18. Ghaneh P, Kawesha A, Evans JD, et al. Molecular prognostic markers in pancreatic cancer. *J Hepatobiliary Pancreat Surg* 2002;9:1–11.
19. Parikh DA, Durbin-Johnson B, Urayama S. Utility of serum CA19-9 levels in the diagnosis of pancreatic ductal adenocarcinoma in an endoscopic ultrasound referral population. *J Gastrointest Cancer* 2014;45:74–79.
20. Humphris JL, Chang DK, Johns AL, et al. The prognostic and predictive value of serum CA19.9 in pancreatic cancer. *Ann Oncol* 2012;23:1713–1722.
21. Shaw VE, Lane B, Jenkinson C, et al. Serum cytokine biomarker panels for discriminating pancreatic cancer from benign pancreatic disease. *Mol Cancer* 2014;13:114.
22. Nicolay A, Lorec A-M, Gomez G, et al. Icteric human samples: Icterus index and method of estimating an interference-free value for 16 biochemical analyses. *J Clin Lab Anal* 2018;32:e22229.
23. de Zwart M, Lausecker B, Globig S, et al. Co-medication and interference testing in bioanalysis: a European Bioanalysis Forum recommendation. *Bioanalysis* 2016;8:2065–2070.
24. Ryan DP, Hong TS, Bardeesy N. Pancreatic adenocarcinoma. *N Engl J Med* 2014;371:1039–1049.
25. Pereira SP, Oldfield L, Ney A, et al. Early detection of pancreatic cancer. *Lancet Gastroenterol Hepatol* 2020;5:698–710.
26. Trikudanathan G, Lou E, Maitra A, et al. Early detection of pancreatic cancer: current state and future opportunities. *Curr Opin Gastroenterol* 2021;37:532–538.
27. Kim J, Bamlet WR, Oberg AL, et al. Detection of early pancreatic ductal adenocarcinoma with thrombospondin-2 and CA19-9 blood markers. *Sci Transl Med* 2017;9:eaah5583.
28. Costello E. A metabolomics-based biomarker signature discriminates pancreatic cancer from chronic pancreatitis. *Gut* 2018;67:2–3.
29. Khan SR, Manialawy Y, Wheeler MB, et al. Unbiased data analytic strategies to improve biomarker discovery in precision medicine. *Drug Discov Today* 2019;24:1735–1748.
30. Krstajic D, Buturovic LJ, Leahy DE, et al. Cross-validation pitfalls when selecting and assessing regression and classification models. *J Cheminform* 2014;6:10.
31. Lipton ZC, Elkan C, Narayanaswamy B. Thresholding classifiers to maximize F1 score. *Mach Learn Knowl Discov Databases* 2014;8725:225–239.
32. Canto MI, Almario JA, Schulick RD, et al. Risk of neoplastic progression in individuals at high risk for pancreatic cancer undergoing long-term surveillance. *Gastroenterology* 2018;155:740–751.e2.
33. Kirkegård J, Mortensen FV, Cronin-Fenton D. Chronic pancreatitis and pancreatic cancer risk: a systematic review and meta-analysis. *Am J Gastroenterol* 2017;112:1366–1372.
34. Sharma A, Kandlakunta H, Nagpal SJS, et al. Model to determine risk of pancreatic cancer in patients with new-onset diabetes. *Gastroenterology* 2018;155:730–739.e3.
35. Pannala R, Basu A, Petersen GM, et al. New-onset diabetes: a potential clue to the early diagnosis of pancreatic cancer. *Lancet Oncol* 2009;10:88–95.
36. Ohno E, Hirooka Y, Kawashima H, et al. Natural history of pancreatic cystic lesions: a multicenter prospective observational study for evaluating the risk of pancreatic cancer. *J Gastroenterol Hepatol* 2018;33:320–328.
37. Kamlage B, Maldonado SG, Bethan B, et al. Quality markers addressing preanalytical variations of blood and plasma processing identified by broad and targeted metabolite profiling. *Clin Chem* 2014;60:399–412.
38. Yin P, Lehmann R, Xu G. Effects of pre-analytical processes on blood samples used in metabolomics studies. *Anal Bioanal Chem* 2015;407:4879–4892.
39. Stevens DA, Lee Y, Kang HC, et al. Parkin loss leads to PARIS-dependent declines in mitochondrial mass and respiration. *Proc Natl Acad Sci U S A* 2015;112:11696–11701.
40. Lehmann R. From bedside to bench—practical considerations to avoid pre-analytical pitfalls and assess sample quality for high-resolution metabolomics and lipidomics analyses of body fluids. *Anal Bioanal Chem* 2021;413:5567–5585.
41. Yin P, Peter A, Franken H, et al. Preanalytical aspects and sample quality assessment in metabolomics studies of human blood. *Clin Chem* 2013;59:833–845.
42. Tonack S, Jenkinson C, Cox T, et al. iTRAQ reveals candidate pancreatic cancer serum biomarkers: influence of obstructive jaundice on their performance. *Br J Cancer* 2013;108:1846–1853.
43. Carayol M, Licaj I, Achaintre D, et al. Reliability of serum metabolites over a two-year period: a targeted metabolomic approach in fasting and non-fasting samples from EPIC. *PLoS One* 2015;10:e0135437.
44. Guo L, Milburn MV, Ryals JA, et al. Plasma metabolomic profiles enhance precision medicine for volunteers of normal health. *Proc Natl Acad Sci U S A* 2015;112:E4901–E4910.
45. Chan A, Prassas I, Dimitromanolakis A, et al. Validation of biomarkers that complement CA19.9 in detecting early pancreatic cancer. *Clin Cancer Res* 2014;20:5787–5795.
46. Brand RE, Nolen BM, Zeh HJ, et al. Serum biomarker panels for the detection of pancreatic cancer. *Clin Cancer Res* 2011;17:805–816.
47. Locker GY, Hamilton S, Harris J, et al. ASCO 2006 update of recommendations for the use of tumor markers in gastrointestinal cancer. *J Clin Oncol* 2006;24:5313–5327.
48. Wolrab D, Jirásko R, Cífková E, et al. Lipidomic profiling of human serum enables detection of pancreatic cancer. *Nat Commun* 2022;13:124.

49. King TC. S8 The IMMray PanCan-d test performance and CA19-9: results from the Blind Validation Study. *Am J Gastroenterol* 2021;116:S4.
50. Kenner BJ, Abrams ND, Chari ST, et al. Early detection of pancreatic cancer: applying artificial intelligence to electronic health records. *Pancreas* 2021;50:916–922.
51. Chari ST, Andersen DK. Metabolic surveillance for those at high risk for developing pancreatic cancer. *Gastroenterology* 2021;161:1379–1380.
52. Sharma A, Smyrk TC, Levy MJ, et al. Fasting blood glucose levels provide estimate of duration and progression of pancreatic cancer before diagnosis. *Gastroenterology* 2018;155:490–500.e2.
53. Oldfield L, Evans A, Rao RG, et al. Blood levels of adiponectin and IL-1Ra distinguish type 3c from type 2 diabetes: implications for earlier pancreatic cancer detection in new-onset diabetes. *EBioMedicine* 2022;75:103802.
54. Chari ST, Maitra A, Matrisian LM, et al. Early Detection Initiative: a randomized controlled trial of algorithm-based screening in patients with new onset hyperglycemia and diabetes for early detection of pancreatic ductal adenocarcinoma. *Contemp Clin Trials* 2021;113:106659.

Received February 1, 2022. Accepted July 14, 2022.

Correspondence

Address correspondence to: Julia Mayerle, MD, Department of Medicine II, University Hospital, LMU Munich, Marchioninistrasse 15, 81377 Munich, Germany. e-mail: julia.mayerle@med.uni-muenchen.de.

CRedit Authorship Contributions

Ujjwal Mukund Mahajan, PhD (Conceptualization: Equal; Data curation: Equal; Formal analysis: Lead; Funding acquisition: Equal; Project administration: Equal; Writing – original draft: Lead; Writing – review & editing: Equal) analysis: Lead; Funding acquisition: Equal; Project administration: Equal; Writing – original draft: Lead; Writing – review & editing: Equal). Bettina Oehrlle, PhD (Resources: Lead). Simon Sirtl, MD (Methodology: Supporting). Ahmed Alnatsha, MSc (Methodology: Supporting; Writing – original draft: Supporting). Elisabetta Goni, MD (Resources: Supporting). Ivonne Regel, PhD (Funding acquisition: Supporting). Georg Beyer, MD (Resources: Supporting). Marlies Vornhülz, MD (Resources: Supporting). Jakob Vielhauer, MD (Methodology: Supporting). Ansgar Chromik, MD (Patient recruitment and follow-up: Equal). Markus Bahra, MD (Patient recruitment and follow-up: Equal). Fritz Klein, MD (Patient recruitment and follow-up: Equal). Waldemar Uhl, MD (Patient recruitment and follow-up: Equal). Tim Falhbusch, MD (Patient recruitment and follow-up: Equal). Marius Distler, MD (Patient recruitment and follow-up: Equal). Jürgen Weitz, MD (Patient recruitment and follow-up: Equal). Robert Grützmann, MD (Patient recruitment and follow-up: Equal). Christian Pilarsky, MD (Patient recruitment and follow-up: Equal). Frank Ulrich Weiss, PhD (Resources: Supporting). Gordian Adam, PhD (Data curation: Equal; Methodology: Equal). John P. Neoptolemos, MA, MB, BChir, MD, FRCS, FMedSci, MAE (Writing – review & editing: Supporting). Holger Kalthoff, PhD (Resources: Supporting). Roland Rad, MD (Resources: Supporting). Nicole Christiansen, PhD (Formal analysis: Supporting). Bianca Bethan, PhD (Data curation: Equal; Formal analysis: Equal). Beate Kamlage, PhD (Conceptualization: Lead; Investigation: Equal; Project administration: Equal; Resources: Equal; Validation: Equal; Writing – review & editing: Equal). Markus M. Learch, MD (Conceptualization: Equal; Writing – review & editing: Equal). Julia Mayerle, MD (Conceptualization: Lead; Funding acquisition: Lead; Investigation: Equal; Project administration: Lead; Visualization: Equal; Writing – original draft: Supporting; Writing – review & editing: Lead).

Conflicts of interest

The authors disclose no conflicts.

Funding

This work was supported by the PePPP Center of Excellence (MV ESF/14-BM-A55-0045/16; ESF MV V-630-S-150-2012/132/133), Deutsche Forschungsgemeinschaft, DFG RE3754/2-1, BE6395/1-1, 413635475, and SFB1321/1 (Project P14, 329628492), Deutsche Krebshilfe, PREDICT-PACA (70113834), Förderprogramm für Forschung und Lehre (FöFoLe, Reg. Nr. 1028), Friedrich-Baur-Stiftung (Reg. Nr. 42/17), Wilhelm-Sander-Stiftung 2019.083.1, and Bundesministerium für Bildung und Forschung 01EK1511A.